RSC Advances

ROYAL SOCIETY OF CHEMISTRY

www.rsc.org/advances

Cite this: DOI: 10.1039/c0xx00000x

www.rsc.org/xxxxxx

ARTICLE TYPE

Electrorheological activity generation by graphene oxide coating on the low-dielectric silica particles

Sang Deuk Kim,[a] Wen Ling Zhang,[a] Hyoung Jin Choi, [a]* Youngwook P. Seo, [b] Yongsok Seo [b]*

Received (in XXX, XXX) Xth XXXXXXXXX 20XX, Accepted Xth XXXXXXXXX 20XX
DOI: 10.1039/b000000x

Recent challenge in the field of electrorheology is to generate or to enhance the elctrorheological (ER) activity of the inactive or lowly active suspension by featuring the core-shell structured particles. Here we illustrate the application of graphene oxide (GO) adsorbed onto the silica particles to make the core-shell structure. The suspension exhibited significant changes in shear viscosity upon the application of an external electric field. The suspension of the core-shell particles also exhibited an occurrence of ER activity enhancement more than an order of magnitude, compared to that of pure silica suspension. The yield stress of this system scales as $\tau_y \propto E^{1.5}$. The dielectric relaxation study revealed that the ER activity was due to the fast occurrence of polarization in the GO-Si suspension. The suspension showed good sensitivity and stability under the electric field. These findings open up the possibilities for design of smart suspensions with high ER responses.

1. Introduction

Electrorheological (ER) fluids are consisted of polarized particles dispersed in insulating medium oils such as silicone oil or mineral oil. Their structural and rheological properties can be reversibly and finely altered by application of an external electric field.[1-5] The polarization attracts the particles one another and instantly (on the order of milliseconds) form solid-like networks along the direction of an applied electric fields.[6-11] The apparent viscosity can be reversibly changed over three to four orders of magnitude at low shear rates. This rapid recoverable response of ER fluids enables them to be good candidates for various applications in mechanical and intelligent devices such as hydraulic valves, dampers, brakes, shock absorbers, vibration attractions, bullet-proof vest, actuators, micro-fluidics gate as well as ER polishing.[12, 13]

To be rheologically active, the suspended particles should be polarized under the electric field. However, fully dried silica microspheres in this study do not undergo much polarization to attract one another in electric fields; hence, they are not useful for ER application. One strategy for induction of ER activity to non-conducting and/or not-easily polarizable particles is coating the surfaces of particles with a more polarizable or conducting material.[14-17] This can enhance the permittivity of the particles in relation to the medium. Because of its high aspect ratio and excellent electrical properties, graphene has attracted a lot of attention.[18] However, pure graphene is not suitable for ER fluid applications because of its high conductivity which leads to electric short circuit,[8] along with its hydrophobicity. In place of pure graphene, graphene oxide (GO) was successfully applied to ER application due to its relatively low conductivity but still high polarization ability.[14(a)] In our recent publication, we have shown that otherwise ER inactive suspensions of microspherical polystyrene (PS) in silicone oil exhibited significant ER activity when coated with small concentrations of GO.[14(b)] This is due to the adsorption of GO which induces polarization to aggregate the GO-PS particles in the presence of the electric field. On the other hand, a suspension of silica particles which is quite abundant and easy to control its size does not show much ER activity at all.[15] Recently, Green and coworkers[16] showed that polydimethylsiloxane (PDMS) mixed with sulfonated polyhedral oligomeric silsesquioxane (s-POSS) exhibited strong ER effect. They also reported that s-POSS/PDMS mixtures and PS (weight fractions ranging from 10 to 20 wt%) showed ER activity which was significantly increased due to dipolar activity associated with preferential adsorption of the s-POSS molecules onto the surfaces of PS fillers as well as the viscosity increases by the PS particles. Thereby, a significant enhancement of the ER response (over 90 Pa at moderate fields) of a sulfonated PS/PDMS based ER suspension was achieved due to the addition of sulfonated POSS.[17] The suspension manifests that the shell or coating of the particles in the suspension is largely responsible for the ER behavior of the suspension. Zhang and Choi[18] also studied that silica nanoparticle grafted GO showed better ER activity than GO alone due to the silica nanoparticle's prevention of GO aggregation.

We report here that GO coated silica particles, otherwise showing poor ER activity, exhibited a significant ER activity at moderate fields. Because silica particle is a commodity material, the cost of processing large quantities of an ER fluid based on this system can be minimized. Also this system exhibit higher viscosities than GO-coated PS suspension system.[14] Such a system would

facilitate easier processing utilization in micro-fluidic applications.

2. Experimental

2.1 Preparation of GO-Si microspheres

GO was prepared by a modified Hummers method, in which 3g of a graphite was dispersed in 210 mL H_2SO_4, and then 210 mL di-water was added slowly to avoid sudden rise of the temperature. Then H_2O_2 was added until the solution color changes to bright brown indicating that graphite was significantly oxidized. The graphite oxide in the solution was exfoliated to become GO by sonication using an ultra-sonication generator (2.8 kHz, 600 W Kyoungil Ultrasonicator Co. Korea). Later, the slurry was separated by centrifugation, washed with 5% HCl and acetone, and then washed with di-water several times until the solution becomes neutral. Finally, the GO was obtained by a freeze-drying method. To graft the amine group on the SiO_2 surface, EDA was used. 3 g of SiO_2 and 20 mL EDA were dispersed in 50 mL H_2O. The mixture was stirred at 80 ^oC for 12 h. The particles were separated by centrifugation. After then, the particles were washed with di-water to remove the excess EDA. Scheme 1 shows the synthesis process of the GO-Si hybrid composite via the chemical grafting reaction.

2.2 Characterization

The morphology of fabricated microspheres was observed by transmission electron microscopy (TEM) (CM200, Phillips, Holland). Microstructure of the chain formation of the ER fluid under an applied electric field was observed using an optical microscope (OM) (U-CMAD3, Olympus, Japan). The chemical composition of fabricated microspheres was checked by Fourier transform infrared spectroscopy (FT-i.r., Bruker, Germany) while their thermal stability was tested using a thermogravimetric analyzer (TGA) (TA Instruments Q50, U.S.A.). The density of the fabricated particles was examined using a gas pycnometer (AccuPyc 1330). The dielectric properties of the suspension were measured using an LCR meter (Agilent HP 4284A) with a frequency range of 20-10^6 Hz which is equipped with a liquid test fixture (16452 A). The measurements were repeated 3 times at 25^oC to ensure reproducibility of the data.

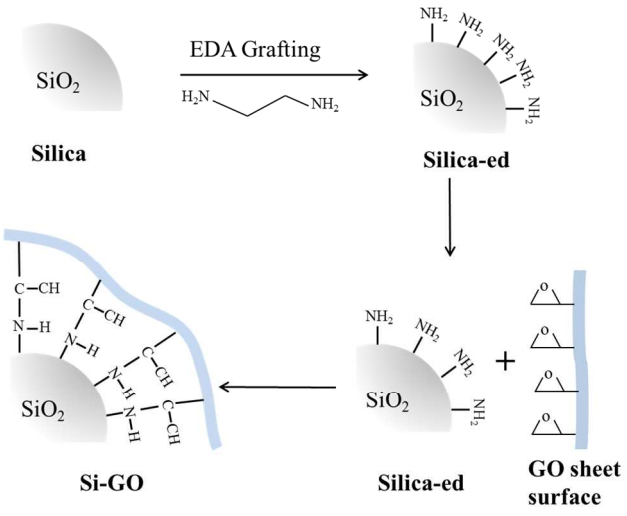

Scheme 1 Schematic diagram of the experimental route to synthesize GO-Si microspheres.

2.3 ER measurement and ER Analysis

The ER performance of the suspension fluid was measured using a rotational rheometer (MCR 300, Physica, Germany) which was attached to a DC high voltage generator (Fug MGH, Germany), and a Couette-type sample geometry with a bob and a cup (CC17, gap distance is 0.71 mm) was used. The flow curves were measured over a wide shear rate range of 1-1000 s^{-1} under varied electric field strength.

An ER fluid can sustain shear stress without flowing in the presence of an applied electric field, because the fluid is known to behave as a plastic material, in which it does not show any deformation unless the shear stress goes over the yield stress to overcome the electrostatic dipole forces which hold the aggregates together (mesostructure). When the shear stress applied is greater than the yield stress, the particle aggregates rupture, and the ER fluid starts to flow. Hence, the yield stress denotes the sharp transition from the solid-like state to the liquid-like state.[3, 17] This behavior of ER fluids (liquid-like to solid-like transition) is represented as the typical Bingham fluid which does not flow at shear stresses below the yield stress and flows above the yield stress. The Bingham equation describes the shear stress change by the following expression,

$$\begin{aligned} \tau &= \tau_{dy}(E) + \eta_{pl}\dot{\gamma} && \tau \geq \tau_0(E) \\ \dot{\gamma} &= 0 && \tau < \tau_0(E) \end{aligned} \qquad (1)$$

where $\dot{\gamma}$ is the shear rate, and η_{pl} is the plastic viscosity which approaches the suspension viscosity at sufficiently high shear rate, and τ_{dy} is the E-dependent dynamic yield stress commonly obtained by extrapolating the shear stress vs. shear rate curve back to the shear stress intercept at a zero shear rate limit.[1,2] The yield stress value obtained using the extrapolation is strongly influenced by the range of shear rates and by the rheological model.[7] Thus, the dynamic yield stress is the yield stress for a completely broken down ER fluid by continuous shearing.[19] On the other hand, ER fluids are naturally thixotropic due to the transition of the microstructure that resists flow-induced particle rearrangement. The yield stress of the ER fluids should be the shear stress required to initiate the shear flow that is initially at rest.[3] It is the yield stress for an undisrupted fluid. Fossum et al.[19] noticed that the yield stress for an ER fluid under continuous shear and under application of a large electric field should be the static yield stress, τ_{sy}, which can differ significantly from τ_{dy}.[1] Most of the previous models such as CCJ model as shown below, De Kee-Turcotte model, the Hershel-Bulkeley model, as well as Bingham model did not correctly predict the static yield stress.[1] The fluid dynamics of the ER fluids should describe the rupture and reformation of the mesostructure (fibrous or columnar structure). Generally the static yield stress is expected to be larger than the dynamic yield stress, but they are comparable magnitude when the stress minimum due to structural change is not evident.[2] The CCJ model was used to describe the structural variation with the shear flow,

$$\tau = \frac{\tau_{dy}}{1+(t_1\dot{\gamma})^{\alpha}} + \eta_{\infty}\left(1+\frac{1}{(t_2\dot{\gamma})^{\beta}}\right)\dot{\gamma} \qquad (2)$$

where t_1 and t_2 are time constants, $\dot{\gamma}$ is the shear rate, τ_{dy} is the yield stress, and η_∞ is the viscosity at high shear rates.[20] The first term on the right hand side represents the shear stress behavior at low shear rates that the shear stress decreases with the shear rate after exhibiting yield behavior. The second term describes the shear thinning behavior at high shear rates. Though this model could describe the deformation behavior of the ER fluids, the yield stress obtained from this model fitting was the dynamic yield stress. We already mentioned about the possible paradox of this model in our previous study.[1,7]

Recently Seo and Seo[1,2,17] proposed an empirical model that combines the nonuniform stress distribution in the context of Bingham fluids with the stress variation due to aligned structure reformation. The Seo-Seo model provides a more realistic account of flows such as structural reformation (destruction and reaggregation of mesostructure). It predicts the static yield stress, τ_{sy}, rather than the dynamic yield stress, τ_{dy}.[1,2] The Seo-Seo model describe the yielding behavior of ER fluids as follows

$$\tau=\tau_{sy}\left(1-\frac{\exp(-a\dot{\gamma})}{1+a\dot{\gamma}^{\alpha}}\right)+\eta_\infty\dot{\gamma} \qquad (3)$$

where τ_{sy} is the static yield shear stress, η_∞ is the shear viscosity, a is the reciprocal shear rate ($a = \dot{\gamma}^{-1}$ for mesostructure deformation) above which the fluid flows with plastic viscosity η_∞ , and α is an empirical parameter, a power-law index used to decide the degree of shear thinning.

3. Results and discussion

GO-adsorbed structure on the silica was confirmed by TEM images as shown in Fig. 1. Compared to circular silica boundary, GO attached silica particle has a rough and rugged surface. FT-i.r. spectra shows that some chemical reaction between GO and silica particles occurred (Fig. 2). The FT-i.r. spectrum of GO in Fig. 2 agrees with our previous results.[14] The OH bond of the GO and C-OH groups can be seen at 3426 and 1397 cm^{-1}. The band centered at 1054 cm^{-1} was associated with the stretching of the C-O band. The stretching vibration of the carbonyl or carboxyl group on GO was observed at 1724cm^{-1}. After the reaction of GO with silica, the characteristic peak of the silica can be seen at 469 cm^{-1} (Si-O-Si stretching). The band at 1105 cm^{-1} is attributed to the (Si-O-C) asymmetric stretching. However, the typical peak of the carbonyl group appears at 1724 cm^{-1}. This proves that the epoxy groups were converted to hydroxyl groups (Scheme 1).

Fig. 3 represents TGA curves of pure silica microspheres, GO-Si hybrid composites and GO. The initial weight loss up to 150°C for GO and GO-Si samples was ascribed to the removal of

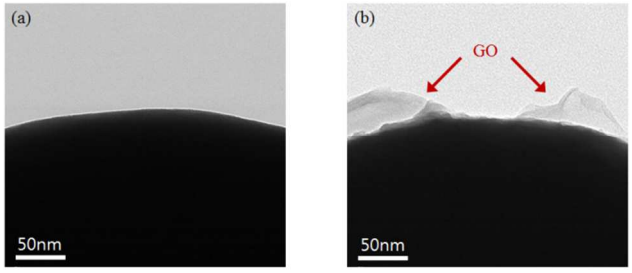

Fig. 1 TEM images of pure silica (a), GO-Si microspheres (b).

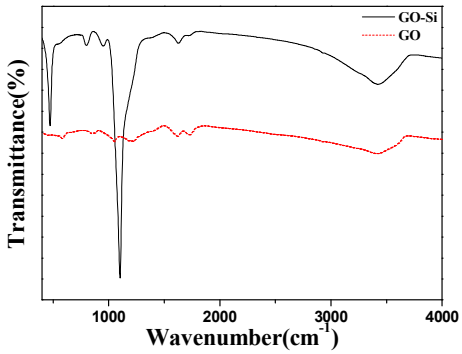

Fig. 2 FT-IR spectra of GO (dotted) and GO-Si microspheres (solid line).

adsorbed water molecules. The weight loss of water at the point of inflection of 125 °C was about 2.0 wt%. Since GO is thermally unstable due to the decomposition of the labile oxygen containing functional groups, it indicates a significant weight loss at 200°C. For the GO-Si microspheres, two characteristic weight losses are between silica and GO indicating that they are less stable than silica particles due to the adhesion of GO.

Optical images of the GO-Si based ER fluid in the presence of an applied electric field are shown in Fig. 4. Without the electric field, the particles were randomly dispersed. When the electric field was applied, the field-induced structures (aggregates of GO-Si) span the electrodes of 300 μm gap and were maintained. Unless the magnitude of the shear stress goes over the yield stress, the fluid behaves as a plastic material of little deformation. Attaching the GO on the silica helps particles floatation to reduce the sedimentation because of reduced density of GO-Si (ρ_{silica}= 2.051g/cm^3, ρ_{GO} = 1.950g/cm^3, and $\rho_{GO\text{-}Si}$ = 2.003g/cm^3).

The ER fluid property of pure silica suspension dispersed in silicone oil was characterized using the rotational rheometer in Fig. 5. The shear stress of pure silica suspension with the external flow does not show much variation with the electric fields due to very weak ER activity. The inset in Fig. 5 shows the fits by the CCJ model and Seo-Seo model, and the vertical line indicates the standard deviations of the data. The CCJ model fit shows Bingham-like behavior whereas the Seo-Seo model fit displays

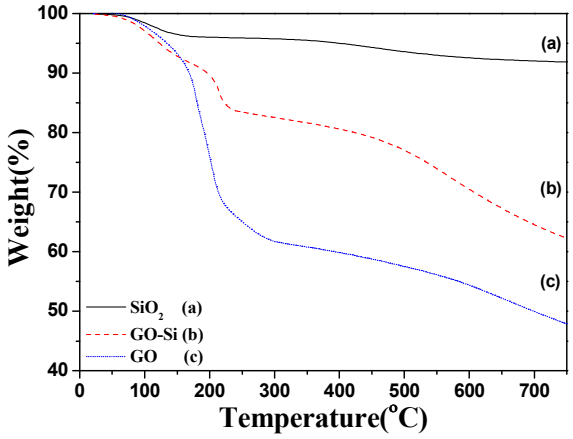

Fig. 3 TGA curves of SiO_2 (a), GO-Si microspheres (B) and GO (c).

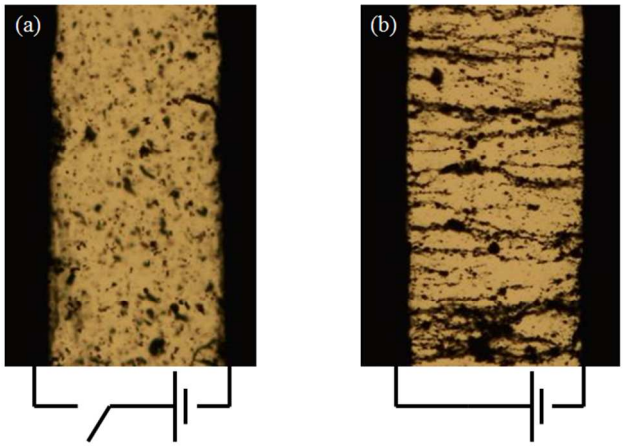

Fig. 4 OM images of the GO-Si microspheres based ER fluid without an electric field (a) and with an electric field (b).

the structural change with the shear rate, though shallow due to weak ER activity, as well as the static yield stress.

The shear stresses are plotted as a function of shear rates in Fig. 6 for the ER fluid of 15 wt% GO-Si suspension. The shear stress increases with the electric field strength. The ER behavior becomes much stronger with the electric field than that of silica particle suspension. At high shear rates, they show trembling behavior (decrease and increase of the shear stress with the shear rate) which becomes more evident with the electric field. The plateau region of the shear stress widens with the electric field because the electrostatic force dominate the hydrodynamic force. If the shear stress overcomes the electric dipole forces that hold the aggregates together, fibrillated chain structures of particles are destroyed and the ER fluid flows. Hence, the shear stress decreases with the shear rate, but the broken structures tend to reform in aligned meso-structure (fibril chains or columns) by the applied electric field. The decrease in the shear stress after reformation arises because the reformed structure are not as complete as those that arise before the application of the shear flow.[1,2] At higher shear rates, the ER fluid exhibits liquid-like behavior in which the ER chains are fully broken. When the electric field strength is high, the ER fluid still exhibits solid-like behavior with a residual stress. The ER fluid then shows a yield stress. The solid curves are computed using the CCJ model and

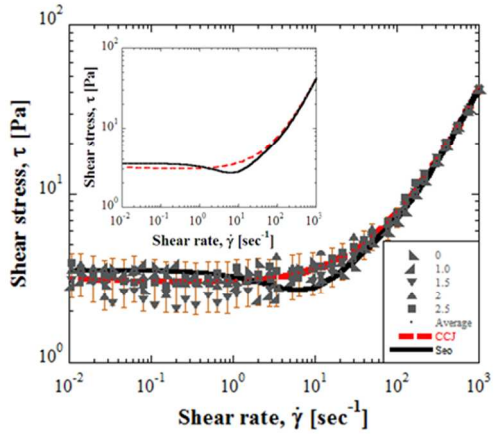

Fig. 5 Shear stress curves *vs.* shear rate for pure silica based ER fluid (15wt% particle concentration).

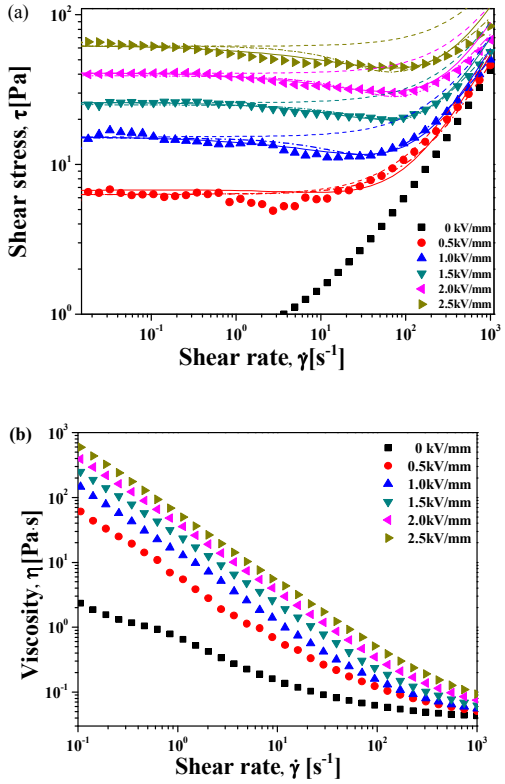

Fig. 6 Shear stress fitted with Bingham model (dash line) and CCJ model (solid line) and SCS model (dash dot line) (a) and shear viscosity (b) curves *vs.* shear rate for GO-Si microsphere based ER fluid (15wt% particle concentration).

the dashed curves are fits to the Bingham model and the dashed and dot curves were calculated using the Seo-Seo model. The Bingham shear stress decreases at low shear rates while the shear stress from the CCJ model increases at low shear rates. The shear stress by Seo-Seo model remains unaffected. However, the values of the yield stress from each model fit were not much different. The fitting parameter values are summarized in Table 1. The yield stress data indicate that the yield stress increases with the electric field. Also the critical shear rates ($\dot{\gamma}_c = a^{-1}$) increases with the field in a consistent manner to show that it is in accord with the strength of the ER fluid. The stress reaches minimum at the critical shear rate due to the competition between the hydrodynamic forces and the polarization forces. In general, the dependency of the yield stress upon the electric field strength can be represented by the power-law relationship ($\tau_y \propto E^m$).[17] When the power-law index m is 2.0, it follows the polarization model, while m=1.5 implies that it corresponds to the conductivity model. The E field dependence decreases from ~2.0 for low fields to ~1.5 for high fields where one reaches the point of diminishing returns. Fig. 7 displays that the yield stress scales approximately as $E^{1.5}$, following the conductivity model.[14] The enhancement of the ER response of the GO-Si suspension is evident from the yield stress.

Also shown in Fig. 6 is the shear viscosity vs. shear rate for GO-Si suspension. Without electric field, the fluid shows quite weakly shear thinning behavior with nominal yield stress. When

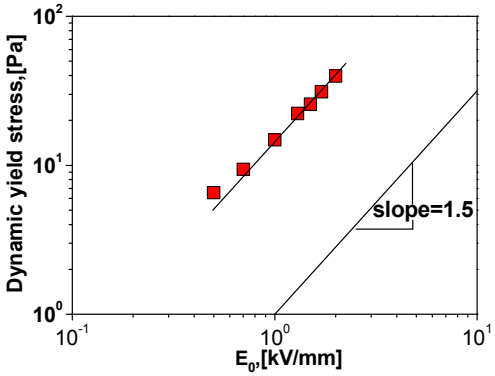

Fig. 7 Dynamic yield stress of the GO-Si microspheres based ER fluid as function of external electric field strengths.

electric fields are applied, the viscosity significantly (more than 2 orders) increases and the fluid flows like a plastic material with yield stress. With the electric field, the suspension forms a solid-like structure from which typical shear thinning behaviors are coming.

The dielectric spectra of the silica particle suspension and GO-Si suspension were examined with a LCR meter in the frequency range, 20-10^6 Hz and are plotted in Fig. 8. GO-Si suspension exhibits faster polarization and higher achievable polarizability due to the addition of GO on the silica. It is quite evident that the increase in the ER response is due to the enhancement of the dipolar activity by GO addition. [14, 15] There are lots of polar groups on the attached GO surface which can be oriented with the applied external electric fields. The orientation of dipoles is in accord with the change of frequency at the low frequency range to increase the dielectric loss whereas the dipoles are unable to follow the change of frequency at high frequency range, thus leading to the appearance of dielectric loss peak. The polarization rate is also important to the ER effect because the polarization rate is related to the stability and reorganization of the ER structure under the simultaneous effects of both electric and shearing fields.[8] To achieve a good rheological behavior, the appropriate polarization rate, corresponding to the relaxation frequency is known to be within 10^2 to 10^5 Hz.[8, 17, 21] A too-slow polarization rate resulted in insufficient particle polarization whereas a too-fast polarization rate easily resulted in the increase of repulsive interaction between particles due to difference between the polarization direction and the direction connecting two particles.[8,17]

In general the ER effect is associated with an interfacial polarization process at the interface between the solid and liquid interphases.[22] The experimental data for dielectric constant (ε′) and dielectric loss (ε″) in Fig. 8 were fitted using the Cole-Cole equation[23] (or Maxwell-Wagner quation[17]) that predicts the complex permittivity of a binary suspension as follows,

$$\varepsilon^* = \varepsilon' + i\varepsilon'' = \varepsilon_\infty + \frac{\Delta\varepsilon}{(1+i\omega\lambda)^{1-\alpha}} \qquad (0 \le \alpha < 1) \qquad (4)$$

Here, $\Delta\varepsilon=(\varepsilon_0-\varepsilon_\infty)$ is the achievable polarizability of an ER fluid related to the electrostatic interaction between particles, ε_0 is the dielectric constant when the frequency ω is close to 0 and is the dielectric constant at a high frequency limit, and the exponent 1-α characterizes the broadness of the relaxation time distribution. The relaxation time, $\lambda = 1/2\pi f_{max}$ reflects the rate of interfacial polarization under the electric field, where f_{max} is the relaxation frequency of the dielectric loss maximum. Higher stress enhancement is achieved when the λ becomes smaller and Δε becomes bigger. The fitting parameter values of α, λ, ε_0 and ε_∞ for GO-Si suspension were estimated as 0.41, 6×10^{-6} s, 1.035 F/m and 0.975 F/m, respectively. The small relaxation time of GO-Si fluid (6×10^{-6} s) indicates that GO-Si suspension responds very quickly (fast polarization) under an electric field to show good ER performance. The large Δε and proper polarization response in the GO-Si fluid induces a strong and stable interaction between particles for higher ER activity.

Viscoelastic behavior of the ER fluid based on GO-Si was tested through the amplitude sweep test followed by a frequency sweep test at various electric field strengths. In the amplitude test shown in Fig. 9, angular frequency was fixed at 6.28 rad/s by the test system. The storage modulus (G′) was observed to be higher than loss modulus (G″) under the same electric field strength. Therefore, the ER fluid performs more elastically showing solid-like behavior. At the low amplitude range, flat area was shown in G′ and G″ curves, indicating a linear viscoelastic region where deformation of structure was reversible. Furthermore, when the electric field strength was higher than 0.5kV/mm, the flat area of G′ and G″ became more wide because solid characteristics of the ER fluids were reinforced by increasing the electric field strength. The structure starts to break down with the increasing strain over 0.015% which is the critical strain limit for the angular frequency measurements. Hence, a strain of 0.01% was chosen for the frequency sweep test. Dynamic oscillation (frequency sweep) test

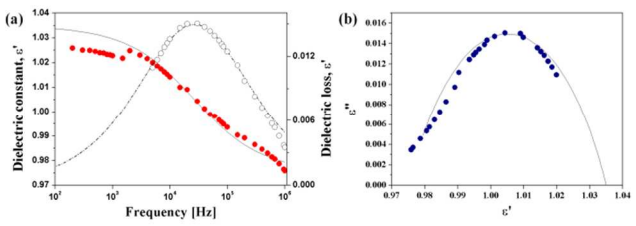

Fig. 8 Dielectric spectra (a) and Cole-Cole fitting curves (b) of GO-Si ER fluid (15wt% particle concentration).

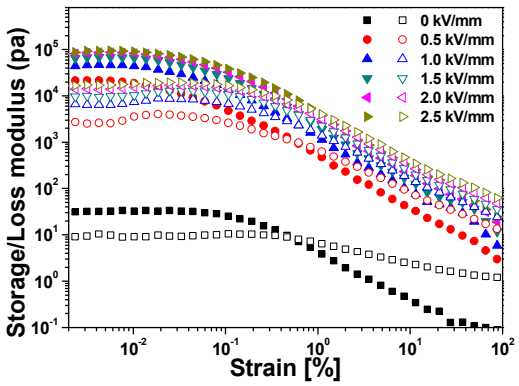

Fig. 9 Amplitude sweep of the GO-Si microspheres based ER fluid (15wt% particle concentration) under various electric field strengths.

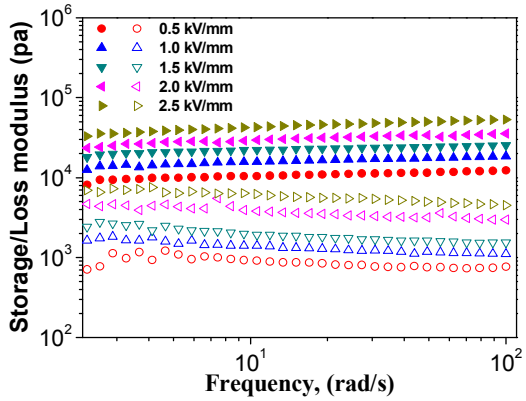

Fig. 10 Frequency sweep of the GO-Si microspheres based ER fluid (15wt% particle concentration) under various electric field strengths.

results are shown in Fig. 10. Storage modulus values, G′, are higher than the loss modulus, G″, through the whole frequency range showing the dominance of elastic property under viscoelastic conditions. Both G′ and G″ values increased noticeably with the electric field strength.

To determine the sensitivity of the ER fluid to an electric field as well as the stability in the relevant electric field, the shear viscosity was measured with various electric field at a fixed shear rate $\dot{\gamma}$=1 and a square voltage pulse (t = 20s). Fig. 11 shows the sensitivity of the ER fluid to an external electric field. Application of an electric field enables the shear viscosity to rise rapidly. The shear viscosity decreases to a zero-field level when the electric field is off. When the applied electric field is weaker than 2kV/mm, the viscosity change is in accords with the electric field on and off to show the step-function response. This is due to the good ER characteristics of GO-Si suspension and good reversibility without deviating hysteresis.[20] At higher electric field, it still shows good response to the electric field but the viscosity varies with time due to the nonlinear viscoelastic behavior. These findings open up the possibilities for design of smart suspensions with high ER responses.

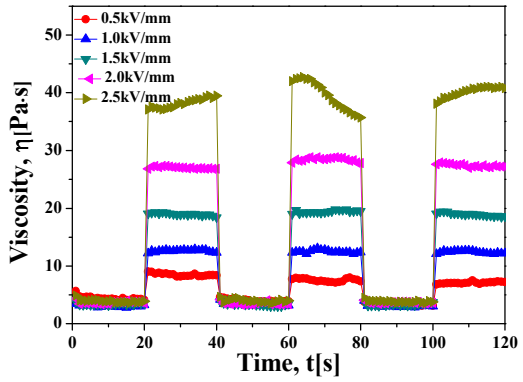

Fig. 11 Viscosity of GO-Si microspheres based ER fluid (15wt% particle concentration) at a fixed shear rate of $1s^{-1}$ in the electric field with a square voltage pulse (t=20s).

4. Conclusions

We have successfully prepared core-shell structure of GO-Si particles by grafting GO on amine-functionalized silica microsphere. The adsorption of dipolar GO particles on the surface of silica particles in a silicone oil medium changes the almost ER-inactive silica suspension to a viable ER fluid. The viscosity changed by 2 orders of magnitude with the application of an electric field. This increase was a few times larger than that exhibited by the suspension of silica nanoparticle adsorbed GO. Though the core material is not conductive, the properties of the shell can provide strong ER properties. Dielectric measurements revealed that GO-Si suspension had a bigger dielectric constant enhancement and a clear dielectric loss peak. This result confirms that GO-shell strengthens the polarizability and subsequently determines the ER activity. The GO-Si suspension had good step-function response without a hysterical response under the strong electric fields. Our result should stimulate further investigations into novel ER suspensions with similar core-shell structures and we expect that our method may be readily applicable to practical ER systems.

Acknowledgements

This study was supported by a research grant from the National Research Foundation, Korea (NRF-2011-0006592) and (NRF-2013R1A1A2057955), the SRC/ERC program (R11 - 2005-065)) and by MIKE (Original Material Technology Program (RIAM No. I-AC12-13(0417-20130067)).

Notes and references

[a] *Department of Polymer Science and Engineering, Inha University, Incheon, 402-751, Korea. E-mail:hjchoi@inha.ac.kr*
[b] *Intellectual Textile System Research Center (ITRC) and RIAM School of Materials Science and Engineering, Seoul National University, Seoul 151-744, Korea. ysseo@snu.ac.kr*

1 (a) Y. P. Seo and Y. Seo, *Langmuir*, 2012, **28**, 3077; (b) J. Wu, T. Jin, F. Liu, J. Guo, Y. Cheng and G. Xu, *RSC Adv.*, 2014, **4**, 29622.
2 (a) Y. Tian, M. Zhang, J. Jiang, N. Pesika, H. Zeng, J. Israelachvili, Y. Meng and S. Wen, *Phys. Rev. E*, 2011, **83**, 011401; (b) Y. P. Seo, H. J. Choi and Y. Seo, *Polymer*, 2011, **52**, 5695.
3 J. B. Yin and X. P. Zhao, *Nanoscale Res. Lett.*, 2011, **6**, art. No. 256.
4 (a) M. Sedlacik, M. Mrlik, V. Pavlinek, P. Saha and O. Quadrat, *Colloid Polym. Sci.*, 2012, **290**, 41; (b) M. Kontopoulou, M. Kaufman, A. Docoslis, *Rheol. Acta*, 2009, **8**, 409.
5 (a) K. P. S. Parmar, Y. Meheust, B. Schjelderupsen and J. O. Fossum, *Langmuir*, 2008, **24**, 1814.
6 (a) M. Kaushal and Y. M. Joshi, *Soft Matter*, 2011, **7**, 9051; (b) F. F. Fang, J. H. Kim, H. J. Choi and Y. Seo, *J. Appl. Polym. Sci.*, 2007, **105**, 1853.
7 (a) H. Orihara, Y. Nishimoto, K. Aida and Y. H. Na, *Phys. Rev. E*, 2011, **83**, 026302; (b) J. Jiang, Y. Tian, Y. Meng, *Langmuir*, 2011, **27**, 5814.
8 (a) J. B. Yin, R. T. Chang, Y. Kai and X. P. Zhao, *Soft Matter*, 2013, **9**, 3910; (b) O. Erol, M. del Mar Ramos-Tejada, H. I. Unal and A. V. Delgado, *J. Colloid Interf. Sci.*, 2013, **392**, 75.
9 M. F. Geist, K. Boussois, A. Smith, C. S. Peyratout, D. G. Kurth, *Langmuir,* 2013, **29**, 1743.
10 R. Tao and Q. Jiang, *Phys. Rev. Lett.*, 1994, **73**, 205.
11 (a) C. L. Li, J. K. Chen, S. K. Fan, F. H. Ko and F. C. Chang, *ACS Appl. Mater. Interfaces,* 2012, **4**, 5650; (b) J. Wang, H. Hu, X. Wang, C. Xu, M. Zhang and X. Shang, *J. Appl. Polym. Sci.*, 2011, **122**, 1866.
12 L. Liu, W. Cao, J. Wu, W. Wen, D. C. Chang and P. Sheng, *Biomicrofluidics*, 2008, **2**, 034103.

13 Q. H. Nguyen and S. B. Choi, *Smart Mater. Struct.*, 2009, **18**, 115020.
14 (a) W. L. Zhang and H. J. Choi, *Chem. Commun.*, 2011, **47**, 12286; (b) W. L. Zhang, Y. D. Liu and H. J. Choi, Zhang, *J. Mater. Chem.,* 2011, **21**, 6916; (c) S. D. Kim, W. L. Zhang and H. J. Choi, *J. Mater. Chem.C,* 2014, **2**, 7541.
15 J. Y. Hong and J. Jang, *Soft Matter*, 2012, **8**, 7348.
16 E. C. McIntyre, H. Yang and P. F. Green, *ACS Appl. Mater. Interfaces*, 2012, **4**, 2148.
17 (a) Y. Yin, C. Liu, B. Wang, S. Yu and K. Chen, *Dalton Trans.*, 2013, **42**, 7233; (b) C. McIntyre, H. Yang and P. F. Green, *ACS Appl. Mater. Interfaces*, 2013, **5**, 8925; (c) B. Wang, C. Liu, Y. Yin, S. Yu, K. Chen, P. Liu and B. Liang, *Compos. Sci. Tech.*, 2013, **86**, 89.
18 P. Nayak, P.N. Santhosh, S. Ramaprabhu, *J. Phys. Chem. C* 2014, **118**, 5172.
19 Y. Meheust, K. P. S. Parmar, B. Schjelderupsen and J. O. Fossum, *J. Rheol.*, 2011, **55**, 809.
20 M. S. Cho, H. J. Choi and M. S. Jhon, *Polymer*, 2005, **46**, 11484.
21 A. Kawai, Y. Ide, A. Inoue and F. Ikazaki, *J. Chem. Phys.*, 1998, **109**, 4587.
22 M. Mrlik, M. Sedlacik, V. Pavlinek, P. Bober, M. Trchova, J. Stejskal and P. Saha, *Colloid Polym. Sci.* 2013, **291**, 2079.
23 H. J. Choi, C. H. Hong and M. S. Jhon, *Int. J. Mod. Phys. B*, 2007, **21**, 4974.